



ELSEVIER

Journal of Non-Crystalline Solids 195 (1996) 188–198

JOURNAL OF
NON-CRYSTALLINE SOLIDS

Effects of water in simulated borosilicate-based nuclear waste glasses on their properties

Hong Li ¹, Minoru Tomozawa ^{*}

Materials Science and Engineering Department, Rensselaer Polytechnic Institute, Troy, NY 12180-3950, USA

Received 1 May 1995; revised 30 August 1995

Abstract

The effects of water on the properties of simulated nuclear waste glasses were investigated. Water content in the glasses was varied by melting under different water vapor pressures and subsequently determined by IR spectroscopy. Water was found to deteriorate chemical durability of the glasses determined by the product consistency test (PCT) using powder specimens but not by the MCC-1 test using bulk specimens. Water in the glasses also decreased the glass transition temperature. By contrast, the effects of water on glass melt properties were smaller. Electrical conductivity changed only slightly, and viscosity remained unchanged within experimental error.

1. Introduction

For isolation of nuclear wastes through the vitrification process, waste slurry is mixed with borosilicate-based glass frit and then re-melted. During these processes, water can enter into the final waste glass. Water in silicate glass can affect many glass properties, including chemical durability [1], glass transition temperature [2–4], viscosity [4,5] and electrical conductivity [4,6]. The effects of water in the simulated nuclear waste glasses on various glass properties, including chemical durability, glass transition temperature, viscosity and electrical conductivity, were investigated.

2. Experimental procedures

2.1. Preparation of glasses with different water contents

Three simulated nuclear waste glasses, CVS2-18, CVS2-52 and CVS2-74, were provided by Battelle Pacific Northwest Laboratories (Richland, WA, USA) for this project. Table 1 summarizes the chemical composition of these glasses as reported by Battelle. The water concentration in these glasses was altered by remelting under various water vapor pressures and subsequently determined by IR spectroscopy.

The as-received glasses were remelted at $1150 \pm 4^\circ\text{C}$ in a Pt crucible using a CM rapid temperature furnace (CM Furnace Inc., NJ, USA), while water vapor was bubbled through the melt with air. Various water vapor pressures (93, 355 and 760 mmHg) were produced by changing the temperature of the

^{*} Corresponding author. Tel: +1-518 276 6451. Telefax: +1-518 276 8554. E-mail: tomozm@rpi.edu.

¹ Present address: Battelle Pacific Northwest Laboratories, Richland, WA, USA.

water bath [7]. The air flow rate was 68.5 ml/min for lower water vapor pressures but was reduced to 32.9 ml/min for 760 mmHg water vapor to prevent the melt from splashing out of the Pt crucible.

The melting furnace was preheated to 1150°C in air and then the Pt crucible, containing about 80 g of crushed, as-received glass, was inserted into the furnace. For the first 15 min, the water vapor was introduced through a Pt tube located just above the melt surface. The tube was then inserted into the melt, introducing water vapor directly into the melt. After 30 min, the Pt tube was pulled back to its original position just above the melt surface, and the melt was fired at this temperature for an additional 20 min. The total melting time was 65 min. The melt was then poured into a copper mold with approximate dimensions of 50 mm × 50 mm × 8 mm, and the resulting glass was immediately transferred to an annealing furnace. The glass was held at 400°C for 30 min and then furnace cooled to room temperature. All the glasses made were homogeneous and free from bubbles. This was verified by examining a piece of glass monolith under a polariscope and an optical microscope.

Water content in the glass samples was determined by IR spectroscopy using plate specimens of 15 mm × 15 mm with various thicknesses. Fig. 1 shows IR spectra for the three as-received glasses, as measured by a Perkin–Elmer 1800 FTIR spectrometer (Perkin–Elmer Corp., KY, USA). The spectra are shifted vertically for clarity. The water concentration in the glass can be determined from the IR absorbance at $\sim 3550\text{ cm}^{-1}$ [4,8,9]. (The second peak at $\sim 2700\text{ cm}^{-1}$ is a combination band of the

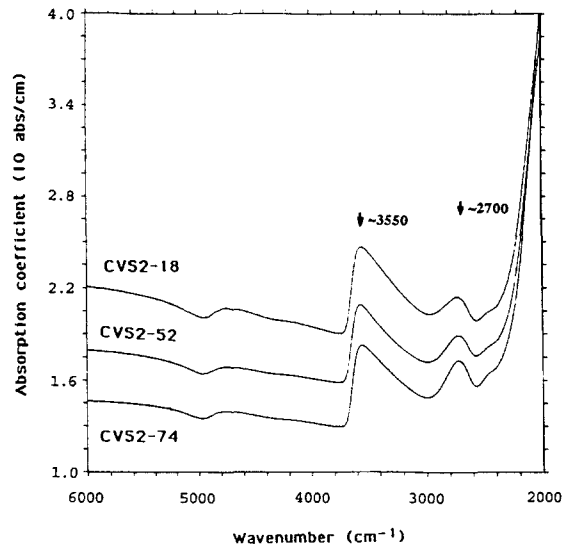


Fig. 1. IR spectra of the as-received glasses (IR absorbance is normalized by the specimen thickness, and the spectra are vertically shifted for clarity).

fundamental B–O vibration modes [10–12].) According to Beer's law,

$$A = \log(I_0/I) = \epsilon Cd = \epsilon' C' d, \quad (1)$$

where A is the hydroxyl absorbance at $\sim 3550\text{ cm}^{-1}$, I_0 and I are the incident and transmitted IR intensities at $\sim 3550\text{ cm}^{-1}$, respectively, after reflection correction, ϵ and ϵ' are the extinction coefficients in $l/\text{mol cm}$ and $l/\text{ppm cm}$, respectively, C and C' are the hydroxyl concentration in mol/l and ppm , respectively, and d is the specimen thickness (cm).

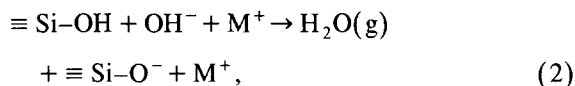
Table 1

Chemical compositions (wt%) of the simulated nuclear waste glasses

Glass oxide	CVS2-18	CVS2-52	CVS2-74	Chemicals
SiO ₂	53.52	60.00	56.60	SiO ₂
B ₂ O ₃	10.53	8.17	7.81	H ₃ BO ₃
Na ₂ O	11.25	4.50	6.64	Na ₂ CO ₃
Li ₂ O	3.75	7.88	7.13	Li ₂ CO ₃
CaO	0.83	0.08	0.79	CaCO ₃
Fe ₂ O ₃	7.19	7.20	3.34	Fe ₂ O ₃
Al ₂ O ₃	2.31	2.33	8.16	Al ₂ O ₃
MgO	0.34	0.09	0.32	MgO
ZrO ₂	3.85	3.85	0.05	ZrO ₂
others	5.92	5.90	9.16	CVS mix ^a

^a CVS mix is composed of various transition metal and rare earth oxides.

To determine the hydroxyl concentration from IR spectra, the extinction coefficient, ϵ or ϵ' , must be known. The weight loss method was used to determine ϵ for these glass compositions. During the dehydration of glass containing alkali, water is believed [3] to diffuse out via the following process:



where M^+ are alkali ions. Thus, the dehydration reaction is accompanied by both specimen weight loss and a reduction in the intensity of IR hydroxyl absorption. The extinction coefficient, ϵ_{OH} (l/mol cm) or ϵ'_{OH} (l/cm ppm), of the IR hydroxyl absorption can be determined [13] by measuring the ratio of the IR hydroxyl absorbance reduction and weight loss. To determine this ratio, a glass specimen was dehydrated at 450°C in a dry nitrogen atmosphere. The sample was periodically taken out of the furnace to measure both its weight and IR spectrum. The accuracy of the weight measurement was ± 0.01 mg, and the effect of adsorbed water on IR spectra was negligible.

2.2. Chemical durability

The chemical durability of the simulated nuclear waste glasses was evaluated using both the MCC-1 and the PCT (product consistency test) methods, and the results were expressed in terms of the normalized elemental mass loss of silicon, boron, lithium and sodium.

2.2.1. MCC-1 chemical durability test

For the MCC-1 [14], three samples with dimensions of 15 mm \times 15 mm \times 0.5 mm were used for each glass having the same water content. The ratio of the specimen surface area to the volume of water (SA/V) was 10 m⁻¹. The initial weight of specimen + water + leach container was recorded, and the initial pH value of ASTM type I water in the PTEF (Teflon) leach container was measured using a 701A digital pH/mV meter (Orion Research Inc., MA, USA).

All specimens were held in a Fisher Isotemp-300 oven, for 28 days at 90 \pm 0.5°C. After 28 days, the specimen + water + container, as well as the glass

specimen itself, were weighed, and the final pH value of leachate was measured.

The concentrations of four elements, silicon, boron, lithium and sodium, in the leachates were analyzed, after filtering through a 0.45 μm membrane, by dc plasma emission spectroscopy, using a Beckman Spectraspan V emission spectrometer (Beckman Instruments, Inc., CA, USA). The dissolved element concentration is expressed in terms of the normalized elemental mass loss, (NL)_{*i*}, [14] given by

$$(\text{NL})_i = C_i/f_i(\text{SA}/\text{V}) \quad (\text{g}/\text{m}^2), \quad (3)$$

where C_i is the concentration of element i in the leachate (g/m³) and f_i is the mass fraction of element i in the unleached specimen. In Eq. (3), f_i values were determined from the compositions of each as-received glass.

2.2.2. PCT chemical durability

Samples were prepared by crushing glass into powder using an alumina mortar and pestle. Powder diameter in the range of 75–150 μm was selected by using 100 and 200 mesh sieves. To remove the fines, prepared powder was washed twice using fresh ethanol in an ultrasonic cleaner. The dried powder sample was mixed with water with a ratio of 10 ml of water per gram of powder [15]. Assuming cubical particles, the mixture had a surface area of sample to the volume of water ratio (SA/V) of ~ 2000 m⁻¹. One sample for each glass of different water content was tested. The PTEF (Teflon) leach containers were placed in a Fisher Isotemp-300 oven for 7 days at 90 \pm 0.5°C. Afterward, specimen + water + container, as well as the glass specimen itself, were weighed and the initial and the final pH values of leachate were measured. The determination of the elemental concentrations for silicon, boron, lithium and sodium in the leachate by plasma spectroscopy followed the same procedures described for MCC-1.

2.3. DSC glass transition temperature

The glass transition temperature, T_g , was measured by the differential scanning calorimetry (DSC) method. A Perkin-Elmer DSC-4 (Perkin-Elmer Corp., KY, USA) was used, and the temperature was calibrated using indium metal. The sample was in

powder form with particle size of about 280 μm and was mechanically sealed in a gold pan. Since the glass transition temperature depends on the heating and cooling rates [16], each sample was cooled from 520°C to 420°C at a cooling rate of 2.5°C/min. The heating rate during the DSC scan was 10°C/min for all measurements. The DSC glass transition temperature, T_g , was determined by the extrapolated onset method [17].

2.4. Viscosity of glass melts

The viscosity was measured using a Brookfield LVT viscometer (Brookfield Engineering Inc., MA, USA), while the melt in a Pt crucible was held in a CM 1300 tube furnace (CM Furnace Inc., NJ, USA). The measurements were conducted at a constant temperature in the range of 950–1250°C at 50°C intervals in air with 93, 355 and 760 mmHg water vapor corresponding to the sample preparation atmosphere. The temperature of the furnace was controlled with $\pm 1^\circ\text{C}$ during the measurement.

The viscosity, η (Pa s), of the glass melt was determined [18] using the relation

$$\eta = (K)(\text{viscometer reading, unitless}) / (\text{spindle rotation speed, rpm}), \quad (4)$$

where K is the cell constant (Pa s rpm) for a given condition and is influenced by the crucible dimensions, the volume of melt and the spindle geometry. In this study, a cylindrical Pt crucible with 50 ml

volume was used, and the volume of glass melt used was about 40 ml. The spindle was immersed into the glass melt to a constant depth, 0.9", from the surface of the melt, which was controlled by using a micrometer.

To determine the cell constant, K , Brookfield standard oils (Brookfield Engineering Inc., MA, USA) with known viscosity values, 12.2 and 103.5 Pa s, were used. These viscosity values are close to those of the glass melts in the temperature range of the measurement.

2.5. Electrical conductivity

The conductivity was determined using a 1689 GenRad RLC Digibridge (QuadTech, Inc., MA, USA). The two electrodes, consisting of Pt wires, were immersed in the glass melt in the Pt crucible held in the CM 1300 tube furnace. The electrical conductivity of the glass melt was measured, using the ac method, in the same temperature range and atmosphere as the viscosity measurement.

The conductivity, σ (S/m), of the glass melts was determined using the method reported by Boulos et al. [19], i.e.,

$$\sigma = Y/R, \quad (5)$$

where Y is the cell constant (m^{-1}) and R is the measured resistance (Ω). R was determined using the complex impedance method [20] in which the dc resistance, R , was taken as the real part of the

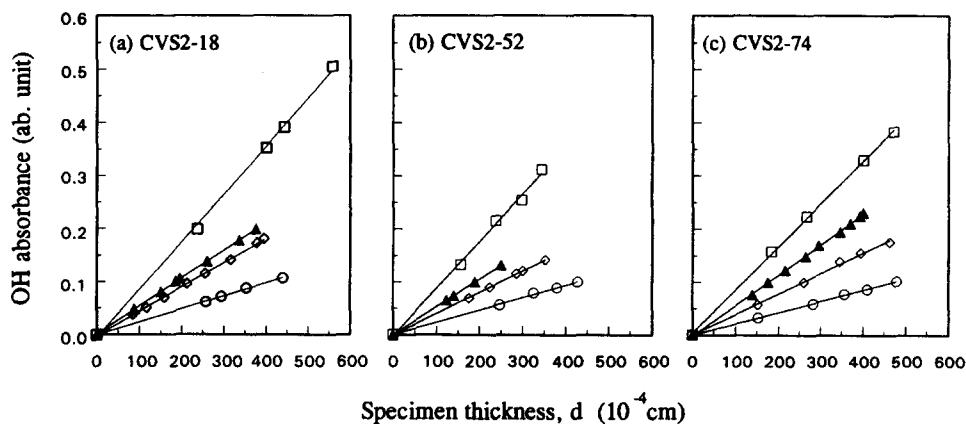


Fig. 2. Hydroxyl IR absorbance as a function of specimen thickness for the glasses with various water contents (water vapor pressures are: \circ , 93 mmHg; \diamond , 355 mmHg; and \square , 760 mmHg. \blacktriangle , as-received glasses).

impedance corresponding to zero imaginary part of impedance.

To determine the cell constant, Y , KCl reference solutions with concentrations of 0.1 and 1.0 D, having known conductivities, were prepared following the method of Parker and Parker [21] (D is for demal, equal to equivalents per dm^3). Frequencies for the electrical measurements ranged from 1 to 100 kHz. The immersion depth of electrodes was 0.7" controlled by a micrometer. The cylindrical Pt crucible with 50 ml volume was used, and the volume of glass melt was about 40 ml. Using the measured resistance, R , and the known conductivity values for these solutions, the cell constant, Y , was then calculated.

3. Results

3.1. Characterization of water content in glass

Fig. 2(a)–(c) show the IR absorbance of hydroxyl versus the specimen thickness for as-received glasses and glasses remelted at 1150°C under various water vapor atmospheres. The linear relation indicates the applicability of Beer's law to the present specimens. The linear regression coefficients were greater than 0.98 in all cases.

Fig. 3 illustrates the loss of the IR absorbance as a

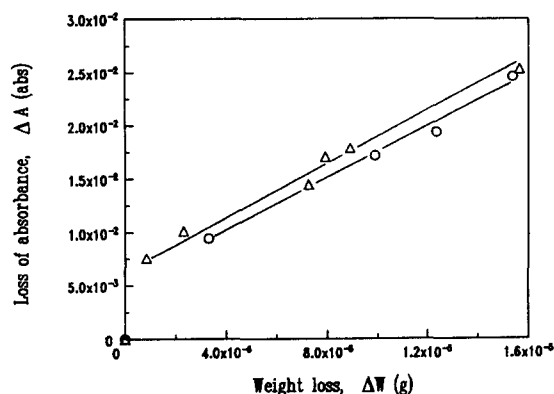


Fig. 3. The change of hydroxyl IR absorbance, ΔA , as a function of the specimen weight loss, ΔW , for the samples dehydrated in dry N_2 at 450°C (○, CVS2-18; △, CVS2-52).

Table 2

Hydroxyl concentration (ppm by wt) in the simulated nuclear waste glasses, hydroxyl absorption coefficient and hydroxyl extinction coefficient

Glass:	CVS2-18	CVS2-52	CVS2-74
<i>OH concentration</i>			
as-received:	4274	3118	3108
94 mmHg ^a :	1976	1376	1146
355 mmHg ^a :	3605	2424	2097
760 mmHg ^a :	7274	5259	4438
$\Delta A / \Delta W$ (abs/g):	1226.6	1713.1	1874.8
ϵ_{OH} (l/mol cm):	7.84	10.99	12.05
ϵ'_{OH} (1/ppm cm):	1.24×10^{-3}	1.70×10^{-3}	1.85×10^{-3}

^a The values represent the water vapor pressures under which these glasses were remelted at 1150°C .

function of the specimen weight loss for CVS2-18 and -52 by dehydration. During dehydration, except for the initial stage, a linear relationship between these two quantities exists. The weight loss followed the parabolic time dependence, indicating the diffusion-controlled loss of volatile. The initial loss of hydroxyl absorbance without weight loss which was observed for the 1 h of dehydration treatment may involve another process than that assumed by Eq. (2).

The extinction coefficients, ϵ_{OH} and ϵ'_{OH} , determined from the linear portion of Fig. 3 and the estimated water contents in the samples are summarized in Table 2. The resulting hydroxyl extinction coefficients, ϵ_{OH} , were found to be smaller than the previously published data: 30 ± 5 l/mol cm for sodium borosilicate glass, 27.5 l/mol cm for Corning 7740 and 28 l/mol cm for Corning 7251 [13]. The difference is probably related to differences in the glass compositions. The estimated water contents show that, under the same melting conditions, CVS2-18 has the highest hydroxyl concentration, while CVS2-74 has the lowest.

The water concentration in glass increased linearly with the square root of water vapor pressure, at relatively low water vapor pressures, as expected [4,22], while it deviated from this trend and was higher than expected at the highest water vapor pressure, 760 mmHg. Similar observations under high water vapor pressure were previously reported for silicate glasses [23,24]. Loss of sodium under a

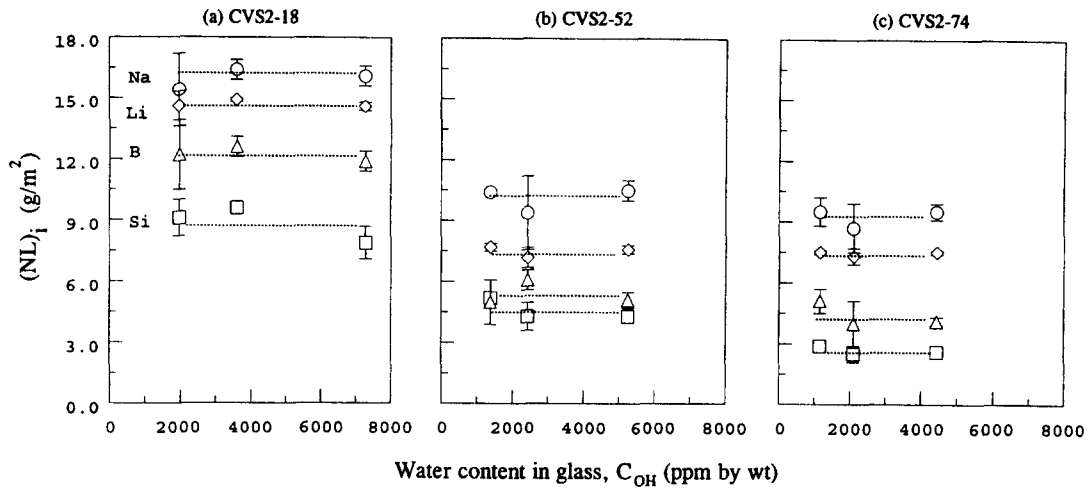


Fig. 4. Normalized elemental mass loss of Na, Li, B and Si determined by 28-day MCC-1 test for the simulated nuclear waste glasses having various water contents.

wet atmosphere during the melting has also been observed [25].

There was a lack of any consistent trends for the as-received glasses, in many glass properties. These as-received glasses have various defects, such as bubbles, and possibly slightly different glass compositions from those remelted in our laboratory. Therefore, the properties of the remelted glasses will primarily be compared.

3.2. Chemical durability

3.2.1. MCC-1

Fig. 4(a)–(c) show the normalized elemental mass loss, $(NL)_i$, for Si, B, Li and Na versus the hydroxyl concentration for CVS2-18, -52, and -74, respectively. For a given glass, the $(NL)_i$ has a general trend of $(NL)_{Si} < (NL)_B < (NL)_Li < (NL)_{Na}$. Among these three compositions, the general trend of $(NL)_i$

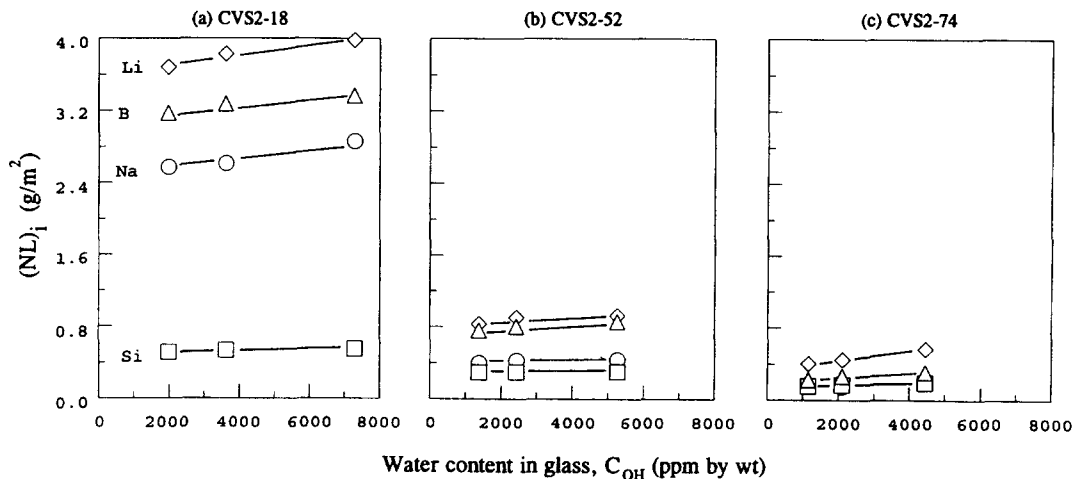


Fig. 5. Normalized elemental mass loss of Na, Li, B and Si determined by 7-day PCT for the simulated nuclear waste glasses having various water contents.

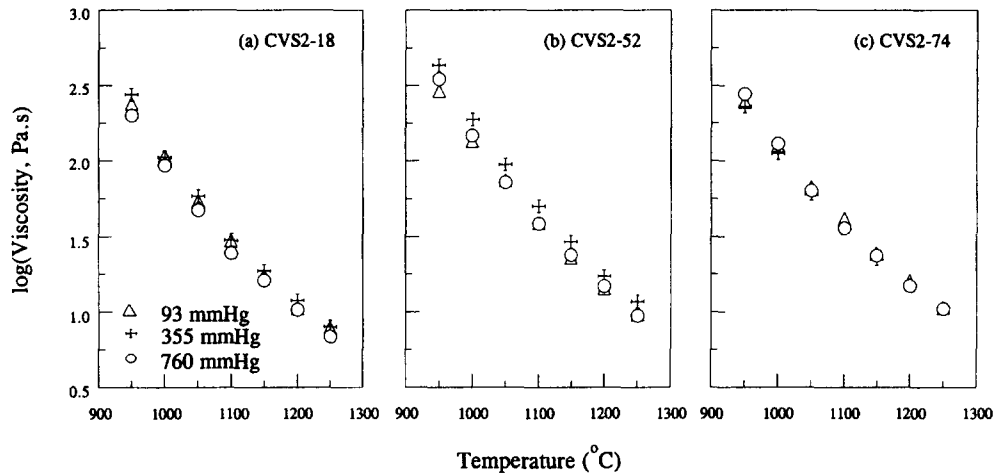


Fig. 6. Viscosity of the glass melts as a function of temperature for the simulated nuclear waste glasses having various water contents.

was $\text{CVS2-18} > \text{CVS2-52} > \text{CVS2-74}$. The results also indicated that the dissolution of each element was mainly influenced by the glass compositions and that the effect of hydroxyl concentration was negligible within experimental error.

The initial pH of type I water was 4.85 ± 0.08 . After the MCC-1 test of the simulated nuclear waste glasses, the pH increased to approximately 9.00 in most cases, while a water blank after the test was only pH 5.39.

During the MCC-1 test, the weight loss of the leachate due to water evaporation was found to be

less than 5 wt%. All glass specimens lost weight slightly as a result of the dissolution. Among the three glasses, CVS2-18 showed the greatest weight loss, $9.4 \pm 0.6 \text{ g/m}^2$, as compared with $5.5 \pm 0.6 \text{ g/m}^2$ for CVS2-52 and $6.6 \pm 0.7 \text{ g/m}^2$ for CVS2-74.

3.2.2. PCT

Fig. 5(a)–(c) show the $(\text{NL})_i$ of Si, B, Li and Na versus the hydroxyl concentration. For a given glass, $(\text{NL})_i$ has a general trend of $(\text{NL})_{\text{Si}} < (\text{NL})_{\text{Na}} < (\text{NL})_{\text{B}} < (\text{NL})_{\text{Li}}$. Among these three glasses, the gen-

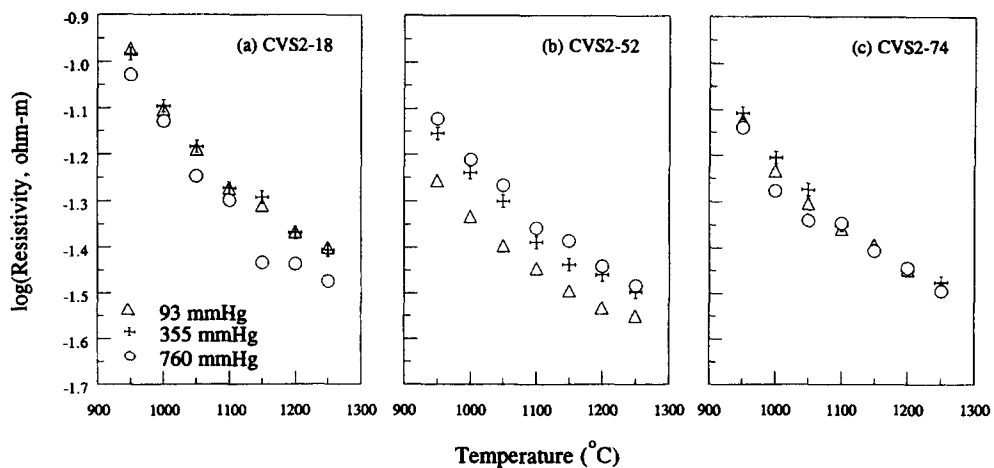


Fig. 7. Electrical resistivity of the glass melts as a function of temperature for the simulated nuclear waste glasses having various water contents.

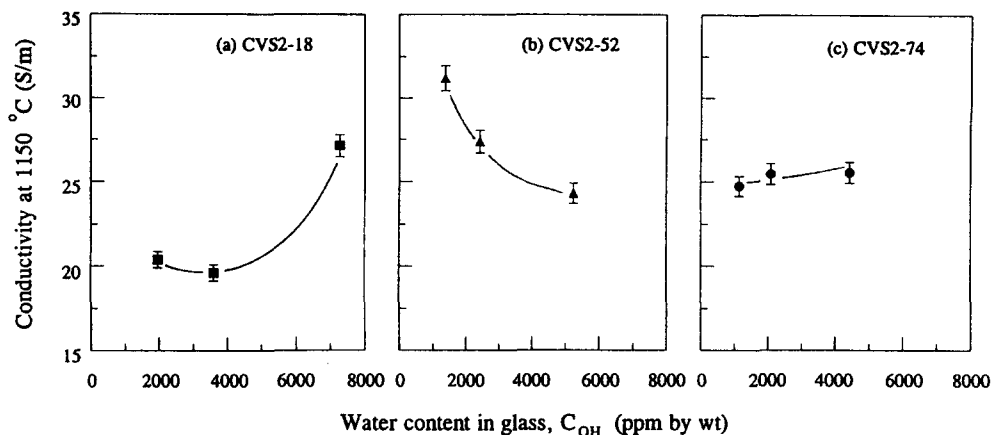


Fig. 8. Electrical conductivity of the glass melts at 1150°C for the simulated nuclear waste glasses having various water contents.

eral trend of $(NL)_i$ was $CVS2-18 > CVS2-52 > CVS2-74$, the same as for the MCC-1 results.

The pH of a blank water was 4.94 at room temperature prior to the PCT. Immediately after mixing the powder with water at room temperature, the pH of the leachate increased to approximately 8.6. The pH values after the PCT were 9.9 for CVS2-18, 9.4 for CVS2-52 and 9.6 for CVS2-74. The final pH of the water blank was 5.48. The weight loss of the leachants during the PCT measurement was less than 1.0 wt%.

3.3. DSC glass transition temperature

Table 3 summarizes DSC glass transition temperatures, T_g , for the glasses having different water content. The error range of the glass transition temperature was $\pm 2^\circ\text{C}$ [17]. The results show that T_g decreases with increasing water concentration in the samples. The effect of water on the change of T_g , however, was rather small for CVS2-52.

Table 3

DSC glass transition temperature ($^\circ\text{C}$) of the simulated nuclear waste glasses with various water contents (heating rate: $10^\circ\text{C}/\text{min}$)

Glass:	CVS2-18	CVS2-52	CVS2-74
94 mmHg ^a :	488	476	474
355 mmHg ^a :	484	476	467
760 mmHg ^a :	471	473	465

^a The values represent the water vapor pressures under which these glasses were remelted at 1150°C.

3.4. Viscosity

Fig. 6(a)–(c) show the logarithmic viscosity as a function of temperature for the three glasses. In general, CVS2-52 had slightly higher viscosities throughout the temperature range than CVS2-18 and CVS2-74. For a given glass and at a specific temperature, viscosity was independent of water content within the experimental error.

3.5. Electrical conductivity

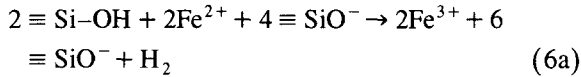
Fig. 7(a)–(c) show logarithmic resistivity as a function of temperature for the ease of comparison with the viscosity data. In general, CVS2-18 has slightly higher resistivities throughout the temperature range employed. Fig. 8(a)–(c) represent the electrical conductivity versus the water concentrations in the glasses at 1150°C.

4. Discussion

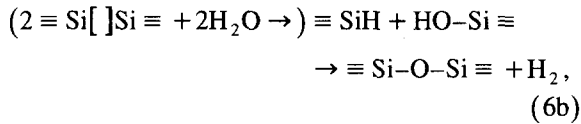
4.1. Extinction coefficient determination

Data in Fig. 3, which were used to determine the extinction coefficient of IR absorbance due to hydroxyl, exhibit non-zero intercepts. It appears that there was an initial decrease in absorbance without a weight loss. This may have been caused by hydrogen loss accompanied by oxidation of transition metal

ion in glass or by annihilation of hydride which was formed by the reaction of oxygen vacancies and water, e.g.,



and

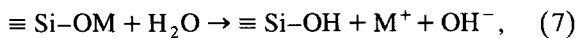


where [] indicates the oxygen vacancy. Both reactions reduce the hydroxyl concentration. It has been reported that hydrogen gas was evolved when silica glasses were heated [26,27]. Because of the light weight of hydrogen, these reactions may not produce detectable weight loss, while they would reduce the hydroxyl absorbance.

4.2. Chemical durability

An influence of water content on the glass dissolution was observed in the PCT, with the higher water content in the glass resulting in slightly greater dissolution of Si, B, Li and Na. However, the influence of water content on the leaching was not detected in the MCC-1 test. The major difference between the two methods was that the (SA/V) value is much higher for the PCT. It is known that the chemical reaction of glass in water proceeds through the processes of (i) ion-exchange between the alkali ions of glasses and hydrogen (or hydronium) in water and (ii) dissolution of the glass network. A higher surface area to the volume of leachant provides more reaction sites and is expected to accelerate these processes.

For the PCT, the initial pH (~ 8.6) of the leachate, immediately after the powder was mixed with water at room temperature, was significantly higher than that for the MCC-1, ~ 4.9 . This is direct evidence for a fast ion-exchange process taking place between the alkali and hydrogen (or hydronium) ions in the PCT. The process can be expressed [28] as



where M^+ is the alkali ion. Also, the final pH increased to nearly 10 after 7 days in the PCT, while

it increased to ~ 9.0 after 28 days in the MCC-1. Other previously reported data of the PCT and the MCC-1 test methods demonstrated that there exists an initial sharp increase in pH level for the PCT which then stabilizes at an even higher level while, for the MCC-1, the pH level increases gradually with time [29–31].

The reaction (7) produces high pH which makes the network dissolution easier. Greenberg and Price [32] previously reported that, at low temperatures (25 and 35°C), the dissolution rate of pure silica remained low and independent of pH below pH 9.0, while, at higher pH, it increased significantly with the pH. At higher temperature (80°C), the pH at which the dissolution rate increases significantly was found to be slightly lower, about 8.5 [33]. This trend also holds for simulated nuclear waste glasses dissolved in pure water [34].

Because of these pH effects, it is anticipated that the concentration profile of alkali elements in the leached layer (or surface layer) would be different for the PCT and the MCC-1. A uniform concentration profile of alkali ions is expected for the PCT because of high pH and fast network dissolution. For the MCC-1, on the other hand, a low alkali surface concentration profile is expected similar to that of silicate glass exposed to pure water [35]. In view of the high initial value of pH 8.6 for the PCT, it is reasonable to assume that, for the PCT measurement, dissolution of the glass network dominates during the most of the test duration after the short, initial ion-exchange stage. For the MCC-1 measurement, on the other hand, the initial pH level of the leachate is low (4.9) and the leaching process is expected to be dominated by ion-exchange during most of the test duration. These hypotheses were further supported by the experimental observation that the concentrations of silicon and boron were significantly higher after the PCT than those after the MCC-1.

In the PCT, the surface layer produced by the initial ion-exchange can be quickly dissolved by the resulting high pH solution, and the network dissolution plays an important role. Water in the glass creates non-bridging Si–OH, making glass weaker and the dissolution rate higher. Therefore, it is reasonable to expect that the chemical durability of glass having higher water content would be poorer in the PCT.

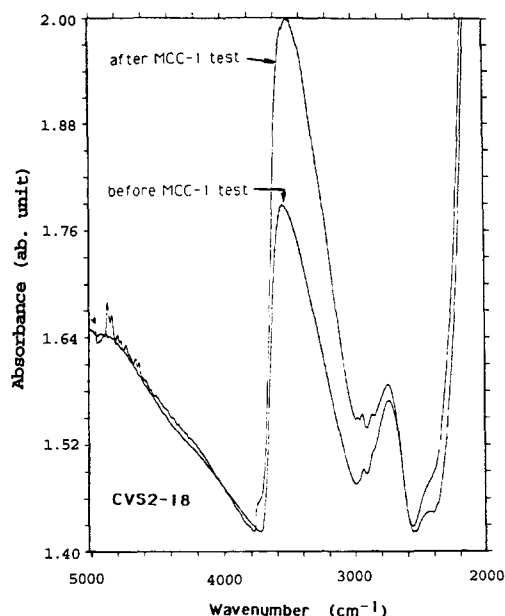


Fig. 9. IR spectra of the CVS2-18 sample before and after the MCC-1 test.

If the network dissolution is taking place in the PCT, the normalized elemental mass loss should be the same for all elements for a given glass. Data in Fig. 5 do not show this. The normalized mass loss of Si is smaller than others. One of the reasons for this discrepancy is reprecipitation of Si at room temperature because of its limited solubility in water.

On the other hand, in the MCC-1, the pH level is lower, and the network dissolution is negligibly small. In this case, a leached layer forms due to the prolonged ion-exchange process at low pH, and this layer contains higher water concentration than that in the bulk. Fig. 9 shows the IR spectra of a CVS2-18 monolith sample before and after the MCC-1 test. An increase in the amount of water is evident after the MCC-1 test. It has been reported that the thickness of the hydration or ion-exchange-affected layer is about 4 μm or less for simulated nuclear waste glasses after the MCC-1 test [36]. The water concentration in the leached layer can then be more than one order of magnitude higher than that in the bulk of CVS2-18 glasses. Similar surface layers with high water contents are also expected to exist for CVS2-52 and CVS2-74 glasses. Since the dissolution proceeds from the leachate/glass interface, the existence of a

significantly higher water concentration in the leached layer should override the effect of the pre-existing water in the glass, even when the network dissolution rather than ion-exchange is an important process. No detectable effect of the pre-existing water content in glass on its chemical durability is, therefore, expected in the MCC-1.

4.3. DSC glass transition temperature

Glass having higher water content showed a lower DSC glass transition temperature. This is consistent with previously reported data on various types of glasses [2–4]. The DSC glass transition temperature obtained under the employed experimental condition corresponds to a viscosity of $10^{11.3}$ Pa s [17].

4.4. Viscosity

Within experimental error, no detectable effect of water in glass on the viscosity of glass melts was observed. In the investigated temperature range, many of the Si–O–Si bonds are broken by high thermal energy, so that additional rupture of the Si–O–Si bridge by water apparently has little further effect. In addition, the effect of water on glass viscosity is known to be strongly dependent on temperature, with the larger effect being observed at lower temperature [4].

4.5. Electrical conductivity

Fig. 8(a)–(c), which illustrate the electrical conductivity versus the water concentration in glass at 1150°C, indicate an interesting trend. At least for CVS2-18 and possibly for CVS2-52, the conductivity initially appears to decrease and then increase with increasing water content in the glass. This water concentration dependence of the conductivity is analogous to previous results on sodium silicate glasses. Conductivity of these glasses at low temperature exhibited a pronounced minimum when plotted against water content [5,6]. From the activation energies of these glasses, the minimum is expected to be shallower and move to the lower water concentration at the higher temperature employed here. The earlier investigation [6] showed that the variation of ionic conductivity by water addition was due to the modi-

fication of alkali ionic mobility rather than to the participation of water-related species such as H^+ .

In the present system, there is an added complication due to the presence of transition metal ions, which can give electronic conduction to the glass, in addition to ionic conduction due to alkali ions. Addition of water to transition metal-containing glass could alter the oxidation state of these ions, which, in turn, can alter the electrical conductivity.

5. Conclusions

Water content in simulated nuclear waste glasses had a measurable influence on the chemical durability of the glasses by the PCT, glass transition temperature and electrical conductivity of glass melts. The effect on both the chemical durability of the glasses by the MCC-1 and viscosity of the glass melts were rather small.

Acknowledgements

The authors gratefully acknowledge the support of Battelle, Memorial Institute, Pacific Northwest Laboratories (Richland, WA, USA) under Grant No. 195074-A-F1. They also acknowledge assistance of Professor C.T. Moynihan of Rensselaer and Dr W.C. Hasz of GE CR&D Center in melt properties measurements. Discussions with Dr. P. Hirma at Battelle and carefully reading of the manuscript by Dr R.D. Sarno and Dr S. Crichton at Rensselaer are appreciated.

References

- [1] M. Tomozawa, C.Y. Erwin, M. Takata and E.B. Watson, *J. Am. Ceram. Soc.* 65 (1982) 182.
- [2] M. Tomozawa, M. Takata, J. Acocella, E.B. Watson and T. Takamori, *Yogyo-Kyokai-Shi* 91 (1983) 377.
- [3] R.F. Bartholomew, *J. Non-Cryst. Solids* 56 (1983) 331.
- [4] H. Scholze, *Glass Ind.* 47 (1966) 622.
- [5] M. Takata, J. Acocella, M. Tomozawa and E.B. Watson, *J. Am. Ceram. Soc.* 64 (1981) 719.
- [6] M. Takata, M. Tomozawa and E.B. Watson, *J. Am. Ceram. Soc.* 65 (1982) 91.
- [7] R.C. Weast, M.J. Astle and W.H. Beyer, eds., *CRC Handbook of Chemistry and Physics*, 56th Ed. (CRC, Cleveland OH, 1975).
- [8] H. Franz, *J. Am. Ceram. Soc.* 49 (1966) 473.
- [9] M.I. Nieto, A. Duran, J.M.F. Navarro and J.L.O. Mazo, *J. Am. Ceram. Soc.* 67 (1984) 242.
- [10] A.S. Tenney and J. Wong, *J. Chem. Phys.* 56 (1972) 5516.
- [11] J.L. Parsons and M.E. Milberg, *J. Am. Ceram. Soc.* 43 (1960) 326.
- [12] G.A. Pasteur, *J. Am. Ceram. Soc.* 56 (1973) 548.
- [13] A.D. Pearson, G.A. Pasteur and W.R. Northover, *J. Mater. Sci.* 14 (1979) 869.
- [14] J.E. Mendel, *Nuclear Waste Materials Handbook*, DOE/TIC-1140 (Pacific Northwest Laboratory, Richland, WA, 1986).
- [15] C.M. Jantzen and N.E. Bibler, *Nuclear Waste Glass Product Consistency Test (PCT)*. Version 3.0, WSRC-TR-90-539Rev.1, Savannah River Laboratory, Aiken, SC (1990).
- [16] C.T. Moynihan, A.J. Easteal, J. Wilder and J. Tucker, *J. Phys. Chem.* 78 (1974) 2673.
- [17] C.T. Moynihan, *J. Am. Ceram. Soc.* 76 (1993) 1081.
- [18] C.T. Moynihan and S. Cantor, *J. Chem. Phys.* 48 (1968) 115.
- [19] E.N. Boulous, J.W. Smith and C.T. Moynihan, *Glastech. Ber., XII Int. Glaskongr.* 56K Bd.1 (1983) 509.
- [20] P.B. Macedo, C.T. Moynihan and R. Bose, *Phys. Chem. Glasses* 13 (1972) 171.
- [21] H.C. Parker and E.W. Parker, *J. Am. Chem. Soc.* 46 (1924) 312.
- [22] A.J. Moulson and J.P. Roberts, *Trans. Faraday Soc.* 57 (1961) 1208.
- [23] J.W. Tomlinson, *J. Soc. Glass Tech.* 40 (1956) 25T.
- [24] C.R. Kurkjian and L.E. Russell, *J. Soc. Glass Tech.* 42 (1958) 130T.
- [25] V. McGahay, PhD thesis, Rensselaer Polytechnic Institute (1992).
- [26] J.J. Murray, R.F. Pottie and R.L. Sander, *J. Mater. Sci.* 8 (1973) 37.
- [27] Y. Morimoto, T. Igarashi, H. Sugahara and S. Nasu, *J. Non-Cryst. Solids* 139 (1992) 35.
- [28] R.J. Charles, *J. Appl. Phys.* 11 (1958) 1549.
- [29] N.E. Bibler and J.K. Bates, *Mater. Res. Soc. Symp. Proc.* 176 (1990) 327.
- [30] W.L. Ebert, *Phys. Chem. Glasses* 34 (1993) 58.
- [31] J.K. McCoy and A.J. Markworth, *J. Non-Cryst. Solids* 89 (1987) 47.
- [32] S.A. Greenberg and E.W. Price, *J. Phys. Chem.* 61 (1957) 1539.
- [33] T.M. El-Shamy and R.W. Douglas, *Glass Technol.* 13 (1972) 77.
- [34] T. Advocal, J.L. Crovisier, E. Vermaz, G. Ehret and H. Charpentier, *Mater. Res. Soc. Symp. Proc.* 212 (1991) 57.
- [35] Z. Boksay, G. Bouquet and S. Dobos, *Phys. Chem. Glasses* 9 (1968) 69.
- [36] D.E. Clark, A. Lodding, H. Odelius and L.O. Werme, *Mater. Sci. Eng.* 91 (1987) 241.